Towards the rational design of cathode and electrolyte materials for aprotic Li–CO_2 batteries: a numerical investigation

Xu Xiao[a], Wenxu Shang[a], Wentao Yu[a], Yanyi Ma[a], Peng Tan[a*], Bin Chen[b], Wei Kong[c], Haoran Xu[d], Meng Ni[d,e*]

[a.] Department of Thermal Science and Energy Engineering, University of Science and Technology of China, Hefei 230026, Anhui, China.
[b.] Institute of Deep Earth Sciences and Green Energy, Shenzhen University, Shenzhen, 518060, China.
[c.] School of Energy and Power, Jiangsu University of Science and Technology, Jiangsu 212003, China.
[d.] Department of Building and Real Estate, The Hong Kong Polytechnic University, Hung Hom, Kowloon, Hong Kong, China.
[e.] Environmental Energy Research Group, Research Institute for Sustainable Urban Development (RISUD), The Hong Kong Polytechnic University, Hung Hom, Kowloon, Hong Kong, China.

*Corresponding authors:
Email: pengtan@ustc.edu.cn (Peng Tan)
Email: meng.ni@polyu.edu.hk (Meng Ni)

Summary: A lithium-carbon dioxide (Li–CO_2) battery offers an effective and efficient approach for the simultaneously CO_2 capture and electrical energy generation. However, the useful guidance for the electrode design and the electrolyte selection is still lacking. Herein, we carry out numerical analyses on the effects of design parameters on the discharge voltage plateau and specific capacity. The developed mathematical model concentrates on the integration of mass transport with the electrochemical reaction to describe the transport and kinetics progresses. After validated by experimental data, the effects of cathode geometries, electrolyte transport properties, and solid product component on the discharge behaviors are detailedly analyzed. The results reveal an

interesting solid product distribution that more is accumulated near two edges and less is in the center of the cathode. For the electrode design, a thinner electrode with a larger porosity is beneficial for a large capacity, and highly active catalysts can diminish the voltage loss and increase the discharge plateau. For the electrolyte selection, it is suggested that higher CO_2 solubility and diffusivity is preferred for the high energy density. Further, the hybrid product component with increasing the carbon content or decreasing the solid Li_2CO_3 content can lead to more reaction sites. This work gives a valuable direction of parameter selection to facilitate the development of Li–CO_2 batteries.

Keywords: Li–CO_2 battery; Numerical simulation; Cathode structure; Electrolyte property; Hybrid product.

1. INTRODUCTION

In the 21st century, the ever-increasing greenhouse gases (mainly CO_2) originated by non-renewable fossil fuel consumption is undoubtedly expediting global warming and rising temperature.[1–4] Currently, carbon dioxide (CO_2) capture, as a hot research top, is commonly transforming CO_2 into chemicals such as gases/liquid CO/CO_2/CH_4 and organic fuels/materials by taking sorbent capture,[5,6] chemical synthesis,[7–9] and electrocatalytic reduction.[10,11] However, sufficient energy supply should be provided at the same time, resulting in “the loss outweighs the gain”. Ever since the proposal of taking CO_2 as the working gas was drawn up in a primary lithium–CO_2 (Li–CO_2) battery in 2013, increasing attention has been attracted for the simultaneous carbon

capture and electrical energy generation.[12–14] The Li–CO_2 battery is an emerging family of next-generation energy storage systems due to the sparkling advantages in both environmental friendliness and high theoretical energy density (1876 Wh kg^{-1}), which accesses to a rational approach to reduce the payload power storage devices for space exploration in submarines or on Mars (96% CO_2 atmosphere). Greatly different from Li–O_2 batteries, CO_2 is used as a cathode fuel, and the aprotic Li–CO_2 battery system is based on the redox chemistry between Li and CO_2 to generate lithium carbonate (Li_2CO_3) and carbon (C).[15,16] Since the hybrid product is scarcely insoluble in the aprotic electrolyte and has low electrical conductivity, the surface of the porous cathode has been gradually growing with the product until drastically covered by a compact passivation film with a certain thickness. In this situation, Li^+ and CO_2 molecules fail to effectively diffuse from the bulk electrolyte to the cathode surface, and electrons hardly go across the passivation film, leading to the low practical capacity during the discharge process. Upon charging, two crucial reaction pathways occur, including the electrochemical self-decomposition of solid Li_2CO_3 with carbon enrichment achieved ($2Li_2CO_3 \rightarrow 4Li^+ + 2CO_2 + O_2 + 4e^-$) or reversible reaction between Li_2CO_3 and amorphous carbon species ($2Li_2CO_3 + C \rightarrow 4Li^+ + 3CO_2 + 4e^-$).[17] Unfortunately, a high charge potential (e.g., > 4.2 V versus Li/ Li^+) is exhibited, which is predominantly caused by the accumulation of insulting Li_2CO_3 with the wide-bandgap feature and high thermodynamic stability, leading to the low round-trip efficiency.[18–20] Furthermore, the potential is such high that side reactions of electrolyte decomposition and carbon-based

electrode corrosion can cause irreversible damage on active surfaces and eventually shorten the cycle life.

To address the aforementioned issues and further improve the electrochemical performance, it is greatly imperative to select appropriate electrolytes, develop advanced cathode materials and high-efficiency catalysts, and design rational porous structure. In the last few years, a series of cathode materials/catalysts to accelerate the sluggish CO_2 reduction and evolution kinetics have been developed in aprotic Li–CO_2 batteries. Zhou et al. introduced graphene and carbon nanotubes (CNTs) cathode to break down the limiting capacity and recyclability barriers,[16,21] which delivered ultrahigh discharge capacities of 14774 mAh g^{-1} and 8379 mAh g^{-1} at the current density of 50 mA g^{-1}, respectively. Dai et al. developed B, N-codoped holey graphene, which further enhanced the reversible capacity to 14996 mAh g^{-1} and showed a superior long and stable cycle life for over 200 times at 1.0 A g^{-1}.[22] Owing to the significance of catalytic activity in the electrochemical reactions, catalysts are dispersed or embedded on cathode surface to facilitate the process. For instance, precious metals Ru and Ir, as well as their composites (e.g. RuO_2, RuP_2, IrO_2), can exhibit satisfactory voltage gaps of 1.44 and 1.77 V over 70 and 50 cycles, respectively.[15,17,18,23–25] The combination of noble metals with transition materials grown on carbonaceous cathode has been proposed to endow durable cycling stability, such as Ru–Cu–G and IrO_2/δ-MnO_2@carbon.[26,27] Under a fixed capacity mode (1000mAh g^{-1}), Ru–Cu–G cathode could remain above 100 times cycling stability at current densities of 200 mA g^{-1} and

400 mA g^{-1}. IrO_2/δ-MnO_2@carbon cathode showed over 300 cycles at 400mA g^{-1} and 200 cycles at 800mA g^{-1}. To acquire low-price catalysts, Zhou et al. developed various transition metal-based catalysts, such as Cu/NG and NiO/CNTs, which possessed high columbic efficiency of 92% and 97.8%, respectively, and good cycling stability of more than 40 cycles could also be achieved.[28,29] Chen et al. utilized Mo_2C@CNT to produce stable intermediates $Li_2C_2O_4$-Mo_2C and reduced the charge potential to be below 3.5 V.[30] Guo et al. reported a soluble redox mediator, binuclear cobalt phthalocyanine (Bi-CoPc), as an alternative to solid catalyst, which could readily-easily oxidize the depositional products and enable the running of 120 cycles without performance decay.[31] Pipes et al. applied an electrolyte additive to induce reversible CO_2 conversion, resulting in remarkable energy efficiency of 98.6% for 30 cycles.[32]

Although aprotic Li–CO_2 batteries have been developed to a certain extent in experimental explorations, the useful guidance for electrode design and electrolyte selection is still lacking. Using mathematical models to describe the working process of the battery and applying numerical analyses on key parameters can not only provide an insightful understanding of the intrinsic mechanisms but also give important design strategies. In Li–O_2 batteries, various modeling and simulation works have been reported, and some intelligent design on the cathode structure has been proposed, such as using gradient porosity[33] and thin electrode[34] to increase the discharge capacity. However, to our best knowledge, the numerical study on the novel Li-CO_2 batteries systems is still absent at present. It is worth noting that owing to the different reaction

mechanisms (e.g., hybrid product of Li_2CO_3 and C) and transport properties of CO_2 in the electrolytes (e.g., solubility and diffusivity), the developed models and numerical results of Li-O_2 batteries cannot be directly applied for Li–CO_2 batteries. To this end, we built a mathematical model of an aprotic Li-CO_2 battery based on macroscopic continuum method and multi-physics coupling in this work. The model validation was carried out through comparing with experimental information in the literature. Subsequently, on account of the valid model, numerical analyses were applied to investigate the impacts of cathode geometrical properties, electrolyte solution transport properties, and solid product component on the discharge performance. This work provides useful guidelines to improve the power and energy density of a Li–CO_2 battery via more reasonable electrolyte selection, electrode design, product component control.

2. RESULTS AND DISCUSSION

2.1 Computational domain and electrochemical reaction

A typical structure of an aprotic Li-CO_2 battery, as shown in Fig. 1, is mainly composed of a CO_2-breathing electrode as the cathode, a lithium metal plate as the anode, and a separator saturated with an aprotic electrolyte. The model contains two domains of the separator (from 0 to L_S) and the cathode (from L_S to L_C) and three boundaries in turn among anode/separator/cathode/ carbon dioxide interfaces (x=0, x=L_S, x=L_C). The dimensionless distance is defined as $\xi = \left(x - L_S\right)/\left(L_C - L_S\right)$.

During discharge, the presence of Li^+ ions travel to the porous cathode and react with the dissolved CO_2 to form solid Li_2CO_3 and amorphous carbon, as expressed in

the following electrochemical reaction:[12,35]

$$4Li^+ + 4e^- + 3CO_2 \rightarrow 2Li_2CO_3 + C \quad (E^0=2.80V \text{ vs. } Li/Li^+) \qquad (1)$$

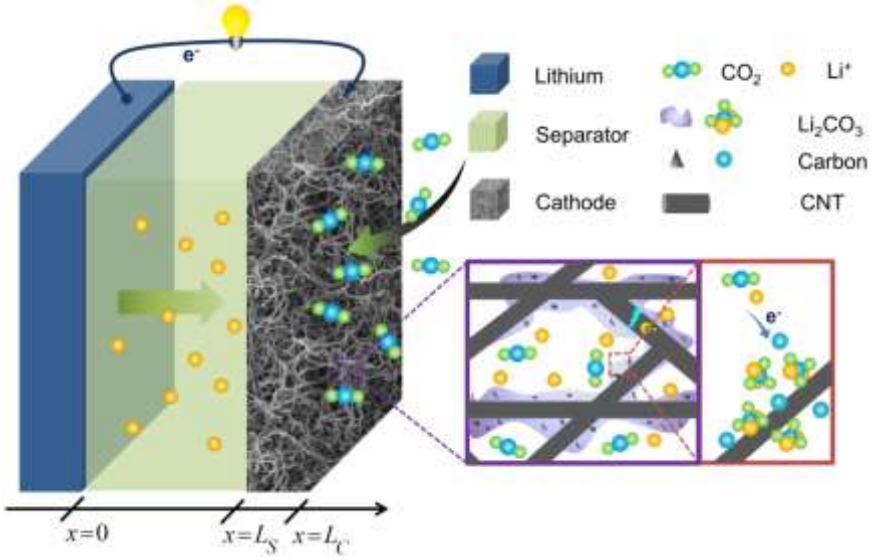

FIGURE 1 Schematic diagram of an aprotic Li-CO_2 battery during discharge. The insets demonstrate reactants transport and the reaction occurs inside the CNTs-based cathode.

The mathematical model was built based on a modified Li-O_2 battery model as demonstrated in the Supporting Information. The values of parameters used for simulations are summarized in Table 1. To validate this model, the initial values of parameters were obtained from an experimental work in which activated carbon nanotubes with a thickness of 500 μm was served as the cathode, and 1 M LiTFSI in TEGDME was used as the electrolyte.[24] The model was developed in a finite element method-based computational platform COMSOL. The maximum time step was set to 0.1 s, and the discharge terminal voltage was 2.2 V. Owing to the applied discharge current density of 50 mA g^{-1}, the discharge capacity should take the specific value (mAh

g^{-1}) and then compare with the experimental data. After validation, the specific values of geometrical properties, rate constant, and electrolyte transport properties were adjusted to discuss the effects on the battery performance.

Table 1. Parameters used in simulation

Parameter name	Symbol	Value	Reference
Initial Li^+ concentration	c_{Li^+}	1000 mol m^{-3}	36
Diffusion coefficient of Li^+	D_{Li^+}	8.98×10^{-10} m^2 s^{-1}	37
Transference number of Li^+	t_+	0.26	38
$\partial \ln f_{\pm} / \partial \ln c_{Li^+}$	-	-1.03	38
Anodic rate constant	k_a	1.11×10^{-14} m s^{-1}	Assumed
Exchange current for anode	i_{a0}	1 A m^{-2}	39
Thickness of the separator	L_s	5×10^{-5} m	40
Porosity of the separator	ε_s	0.87	41
Ionic conductivity of the electrolyte	κ	0.03 S m^{-1}	37
Initial CO_2 concentration	c_{CO_2}	120 mol m^{-3}	12,45
Diffusion coefficient of CO_2	D_{CO_2}	2.32×10^{-10} m^2 s^{-1}	42
Thickness of the cathode	L_c	5×10^{-4} m	
Porosity of the cathode	ε	0.907	
Conductivity of the cathode	σ	30 S m^{-1}	34
Specific surface area of the cathode	a	9.4×10^7 m^2 m^{-3}	
Solubility of Li_2CO_3	$c_{Li_2CO_3}$	0.27 mol m^{-3}	Assumed
Electrical resistivity of Li_2CO_3	R_s	1.0×10^{10} Ω m	Assumed
Density of Li_2CO_3	$\rho_{Li_2CO_3}$	2,110 kg m^{-3}	
Molecular weight of Li_2CO_3	$M_{Li_2CO_3}$	38.94 g mol^{-1}	
Density of carbon	ρ_C	2,260 kg m^{-3}	
Molecular weight of carbon	M_C	12.01 g mol^{-1}	
Operating temperature	T	298.15 K	

2.2 Model validation

As shown in Fig. 2, the simulated discharge voltage curve is compared to the

reported experimental data at the same current density with a terminal voltage 2.2 V.[24] In the experiment, a 500 μm-thick cathode with a three-dimensional cross-linked structure delivered a discharge capacity of 3570 mAh g^{-1} in a CO_2 atmosphere. The voltage curve calculated by our model shows a discharge voltage plateau at around 2.50 V, which agrees well with the experimental result. Owing to the accumulation of insoluble and insulating Li_2CO_3 inside the porous cathode that hinders the flux of gas, ions, and electrons, the voltage keeps decreasing and eventually leads to a sudden drop at nearly terminal voltage due to the greatly increased concentration polarization.[43] This phenomenon is consistent with the experimental observation, and the calculated capacity is 3485 mAh g^{-1}, very close to the experimental value. Thus, the results validate the present model for further numerical analyses.

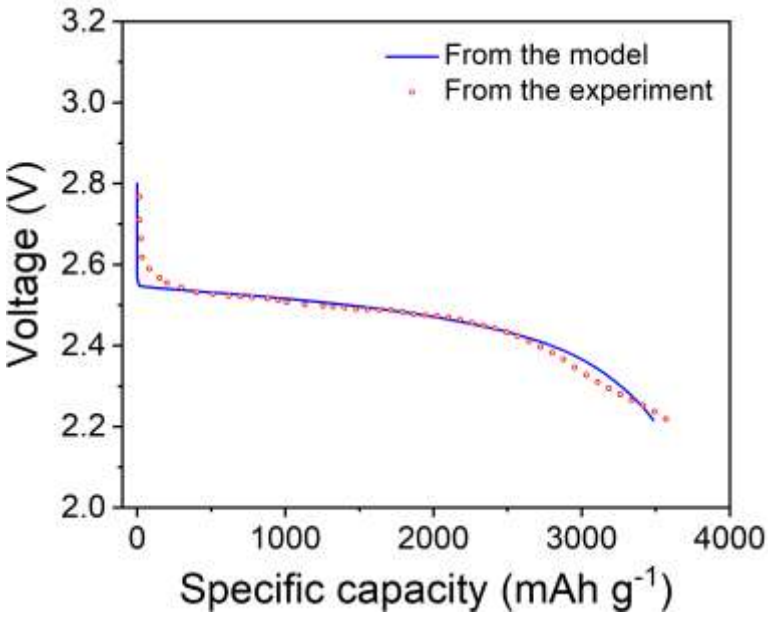

FIGURE 2 The comparison between the simulated discharge voltage curve and the experimental data with a cut-off voltage of 2.2 V.[24] The values of all parameters used

in the model are listed in Table 1.

To obtain an insightful investigation on the transport process during discharge, the concentration of Li^+ ions and CO_2 at various discharge states are investigated. For the distribution of the Li^+ concentration in the cathode, as shown in Fig. 3a, it is apparently decreasing from the separator/electrode interface to the electrode/gas interface, creating the concentration gradient of Li^+ with the discharge goes on. For the concentration of CO_2, as shown in Fig. 3b, it begins to transport and is consumed at the feeding gas side, which diffuses further in the cathode filled with the liquid electrolyte due to the high solubility of carbon dioxide. Generally, the porosity of the cathode in a lithium-oxygen battery decreases from the open to the inner side after discharge due to the limited oxygen solubility. Interestingly, the porosity in this case falls predominantly at both the separator and the gaseous sides of the cathode, but is relatively less in the center, as clearly indicated in Fig. 3c. The utilization ratio of the medial side is higher than lateral side. In addition, the porosity changes from 0.907 to 0.3 owing to the solid products coated on the surface electrode. While similar phenomena have also been reported.[44–46] The reason is that the concentrations of reactants (i.e. CO_2 and Li^+) have great effects on the reaction rate, which then determinate the deposition of Li_2CO_3 on the active sites. As the degree of discharge deepens, the available pore spaces are increasingly occupied with continuously growing solid products so that residual channels are narrow enough, leading to high transport resistant. Thus, the diffusion barrier is the major reason why the sudden death occurs at the end of discharge. In addition, solid products tend to be

tightly stacked with each other and their interaction conduces a compacted film with insulating properties, resulting in greatly decrease active sites.

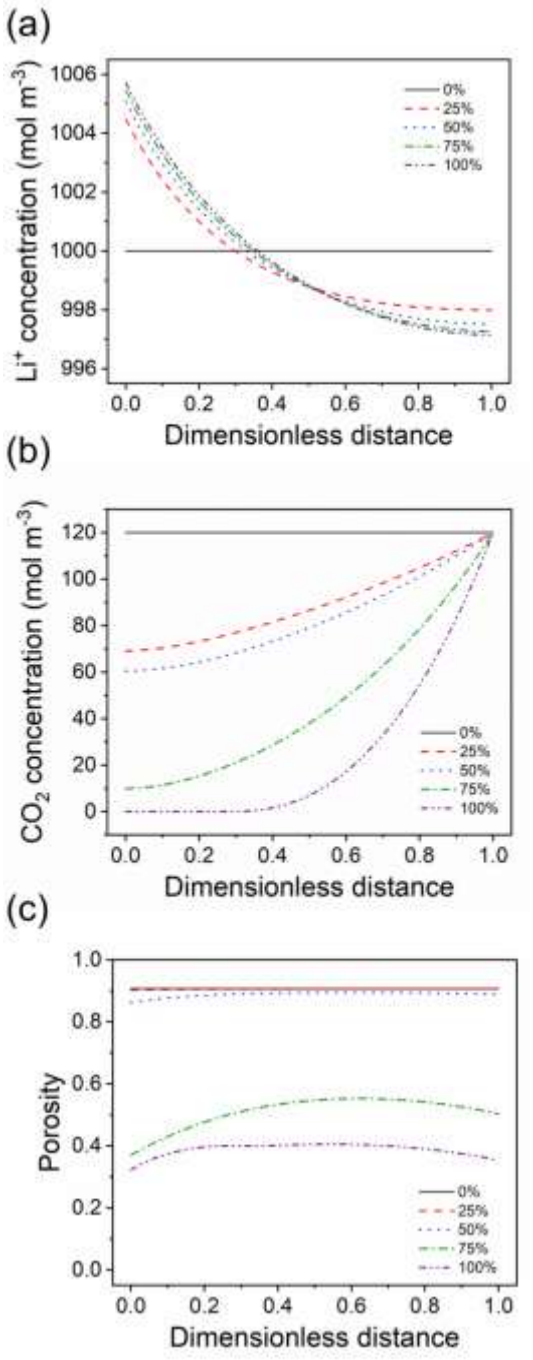

FIGURE 3 Local concentration of (a) Li^+ ion and (b) CO_2 molecule, and (c) porosity distribution in the cathode at different discharge states.

2.3 Effects of cathode properties

Since the cathode has a close correlation with the discharge performance, it is indispensable to take the geometrical factors including the thickness and porosity into consideration. To study the effects of thickness and porosity of the cathode, we employed the single variable method by changing the corresponding value applied in the model to get qualitative results on the battery performance. With regard to a specific cathode material, changing its geometry (e.g., thickness and porosity) is bound to induce the active material loading. Hence, it is more reasonable that using the mass current density (100 mA g^{-1}) instead of the surface area (mA cm^{-2}) to counteract the changes of loading. Practically, various cathode materials with different activity and geometrical size, including the thickness, void volume, and pore structure, have different impacts on the discharge performance, which will be revealed in this section.

2.3.1 Effects of geometry

As demonstrated in Fig. 4a, the voltage-capacity curves on discharge change with different cathode thicknesses. By decreasing the thickness from 500 μm to 350 μm and even 200 μm, there is a clear trend to increase in the specific capacity to 4396 mAh g^{-1} and 5088 mAh g^{-1}, respectively. Nevertheless, the capacity further increases to 5309 mAh g^{-1} at the thickness of 50 μm, and a similar evolution of the voltage plateau is also found. Noteworthy, Scott et al. and Zhao et al. reported such a similar result that a slightly thinner electrode compared with a thick one (e.g. 500 μm) is favourable to accelerate the transport rates of Li^+ and CO_2 in an organic electrolyte, which are

effectively utilize the active materials of the porous cathode.[34,41] In addition, the implication in Eq. S2 is that the cathode thickness will affect the electrochemical reaction and lead to non-uniform distribution in the whole cathode. As the discharge process proceeding, solid hybrid products (Li_2CO_3 and C) are gradually generated, changing both the CO_2 concentration and the porosity. Evidently, to observe synchronous results of the CO_2 concentration and the void space utilization at different thicknesses, the results at the final discharge stage are obtained. As indicated in Fig. 4b, a thinner cathode makes a contribution to shortening the residence time on CO_2 crossover in the electrolyte, which means reducing the gaseous transport resistance. Accordingly, the utilization of the porous cathode increases by the decrease of thickness (Fig. S1). From these results, a strategy is put forward that a thinner cathode is beneficial for high discharge voltage plateau and specific capacity (mAh g^{-1}). It is worth noting that the practical capacity (mAh) depends on the accumulation of solid products, and a thick one may offer more spaces. Thus, an optimal thickness of the electrode should balance the specific capacity (mAh g^{-1}) and the practical one (mAh).

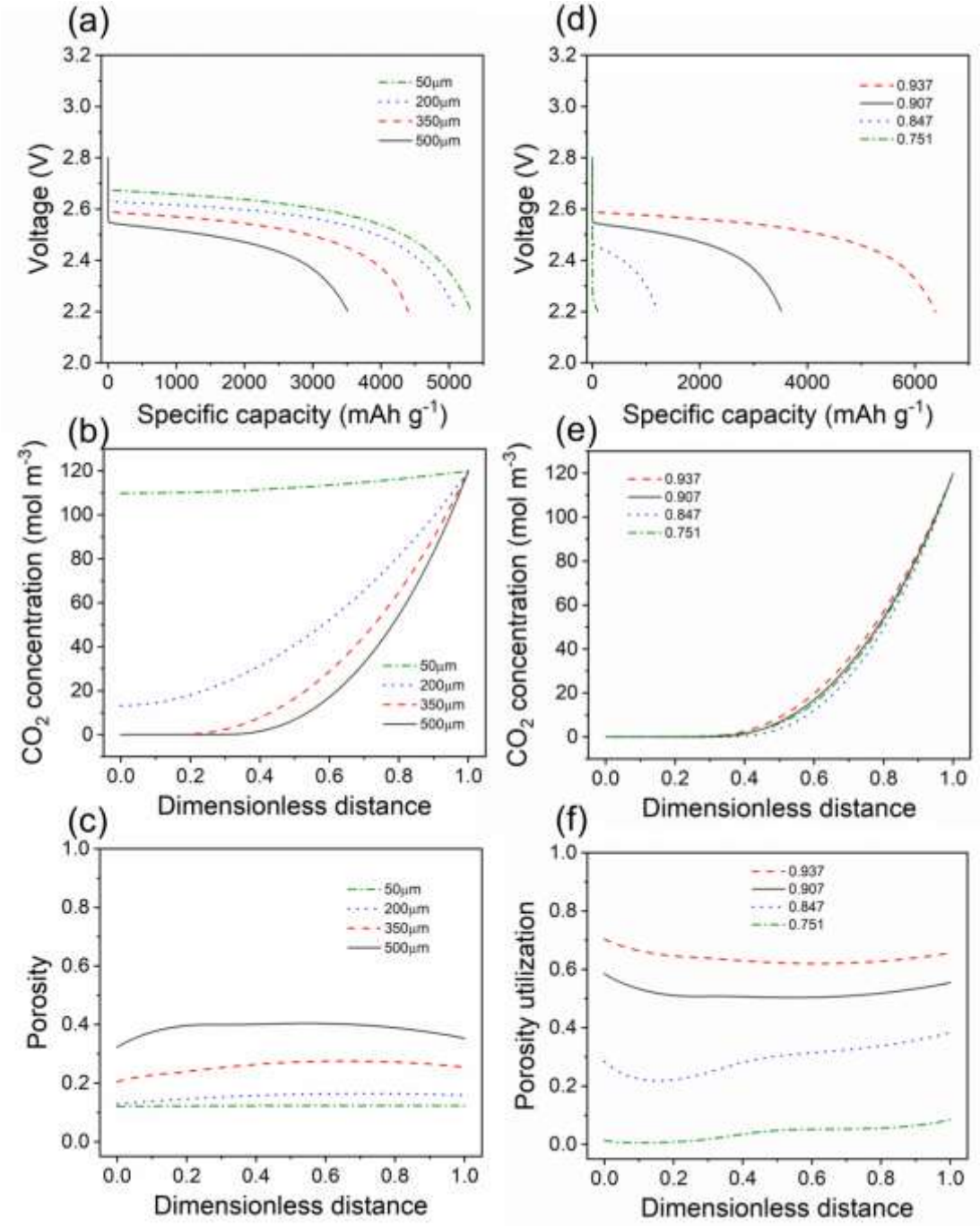

FIGURE 4 Effects of cathode thickness and porosity on the discharge performance, respectively: (a, e) discharge voltage-capacity curves; (b, d) concentration of CO_2, (c) porosity distribution, and (f) the porosity utilization profiles at the end of discharge. The carbon dioxide concentration in electrolyte is 120 mol m^{-3} and the porosity of cathode is 0.907 initially.

As indicated from the material balance equation in Eq. S1, the solid product, Li_2CO_3 mixed with C, stack up and get thicker in the porous channel of the cathode. From Fig. 4d, the voltage-capacity curves vary with different porosities. When increasing/decreasing the porosity, the specific capacities and the voltage plateaus exhibit an opposite trend. The cathode porosities ranged from 0.937 to 0.751 make the capacities change from 6379 mAh g^{-1} to 351 mAh g^{-1}. The similar phenomenon is also found by Tan et al. in a Li-O_2 battery system.[47] As demonstrated in Fig. 4e, the CO_2 concentration distribution at different porosities is almost the same at the end of discharge, indicating that the concentration polarization is a negligible reason for the termination of discharge. Fig. 4f shows the utilization of the void space by solid products at different porosities. Based on the specific microstructure of carbon nanotubes, the larger porosity can provide more spaces for products accumulation. Finally, the lacking of gas/ion/electron transfer, active sites, and storage space terminates the electrochemistry. In a word, choosing a cathode with a large porosity can significantly promote the storage of solid products and achieve a high specific capacity.

2.3.2 Effect of catalytic activity

The reported Li-air batteries usually suffer from high voltage gaps and low efficiency. When it comes to Li-CO_2 batteries, searching for active materials and enhancing the kinetics rate of CO_2 reduction reaction (CORR) is significant. In order to investigate the substantial effects of various catalysts on the discharge capacity, the initial cathodic rate constant (2.38×10^{-32}) is altered to 2.38×10^{-30} and 2.38×10^{-28},

respectively. Specifically, the initial one is the pristine electrode decorated with no catalysts, on the contrary, the others match different catalysts. As can be seen from Fig. 5, the discharge voltage plateau evidently increases with exponential growth in the reaction rate, which is originated by the reduction of voltage loss, whereas the capacity changes slightly. In this regard, the specific capacities with or without effective catalysts are different from previous research, from which different types and loadings can change the active sites. In addition, when design and fabricate cathode, it is possible to enlarge pore size and even open the closed-pores, which will achieve a distinct discharge response. Moreover, the product morphology may change by the addition of catalysts, including spherical particles,[48] needle-like,[24] flake-like,[49] plate-like[50] and even film-like.[17] Thus, figure out the relationship between the product morphology and the reaction rate will be greatly helpful to improve the current model.

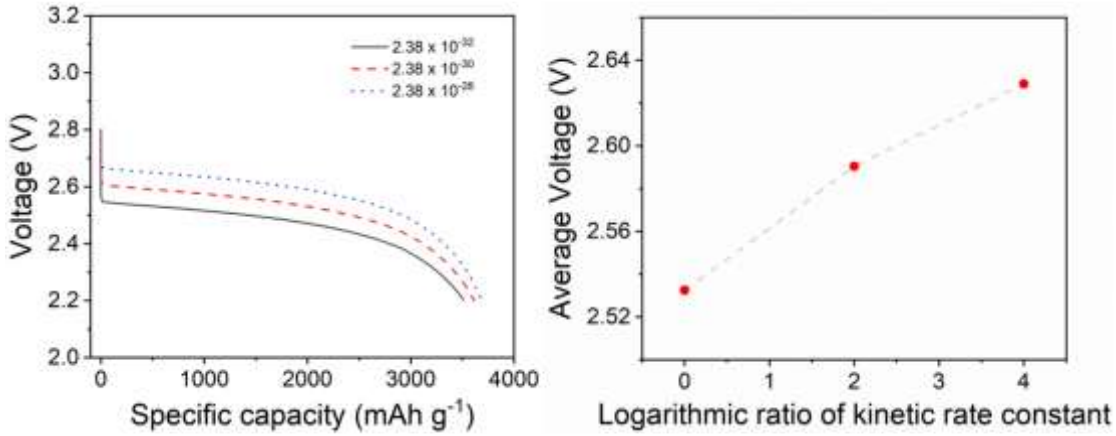

FIGURE 5 Effects of catalytic activity on the discharge performance: (a) discharge voltage curves; (b) average discharge voltages plateau at different reaction rates (the initial one is 2.38×10^{-28}).

2.4 Effects of electrolyte transport properties

Although the detailed mechanisms of CO_2 electrochemical reduction and evolution reactions have not been revealed there is no doubt that the electrolytes have a significant effect.[31,32,51] Since the concentration of Li^+ ions almost keeps a constant value (~1 M) throughout the whole discharge process, the concentration of CO_2 turns to be a major factor in limiting the discharge rate and capacity. Herein, figure out the detailed relationship between the transport properties of CO_2 and the discharge performance, in particular, solubility and diffusivity, is crucial for the selection in suitable electrolytes. In this section, the solubility and diffusivity of CO_2 are assumed to be independent variables, and the respective roles in the discharge behaviors are thus analyzed.

2.4.1 Effects of carbon dioxide solubility

As can be seen from Fig. 6a, when the solubility of CO_2 varies from 100 to 120 mol m^{-3}, the specific capacity is growing remarkably from 3174 to 3510 mAh g^{-1} with an increase of 10.6%; however, the voltage platform changes slightly from 2.56 to 2.57 V. With the solubility increasing, a slight voltage change (Eq. S10) is converted to apparent changes in mass transport and kinetics by an exponential magnification (Eq. S11), and a higher capacity reveals more products accumulated in the porous cathode. With further increasing the solubility to 160 mol m^{-3}, the voltage plateau and the capacity increase to 2.58 V and 3833 mAh g^{-1} (9.2% compared to 3510mAh g^{-1}), respectively. From Fig. 6b, the higher solubility causes a higher overall concentration,

and the residual CO_2 can reach the deep of the cathode at the end of discharge. The porosity distribution is shown in Fig. 6c. Interestingly, the product distribution distributes differently at different solubility. Generally, solid products are eager to generate on both sides, especially the inner side of the cathode. However, an increasing solubility tremendously facilitates to shape the gradient away from the inlet side, which can take full advantage of the available pores deep in the cathode rather than the CO_2-breathing side. After the transport channels are confined by accumulated products, residual gas continues to react with abundant Li^+ ions until the other side is fully blocked. As a result, higher CO_2 solubility will be favorable for the increase in both the voltage platform and the discharge capacity, which is possible to be a novel approach to lower the overpotential during discharge through increase the operating pressure to increase the solubility.

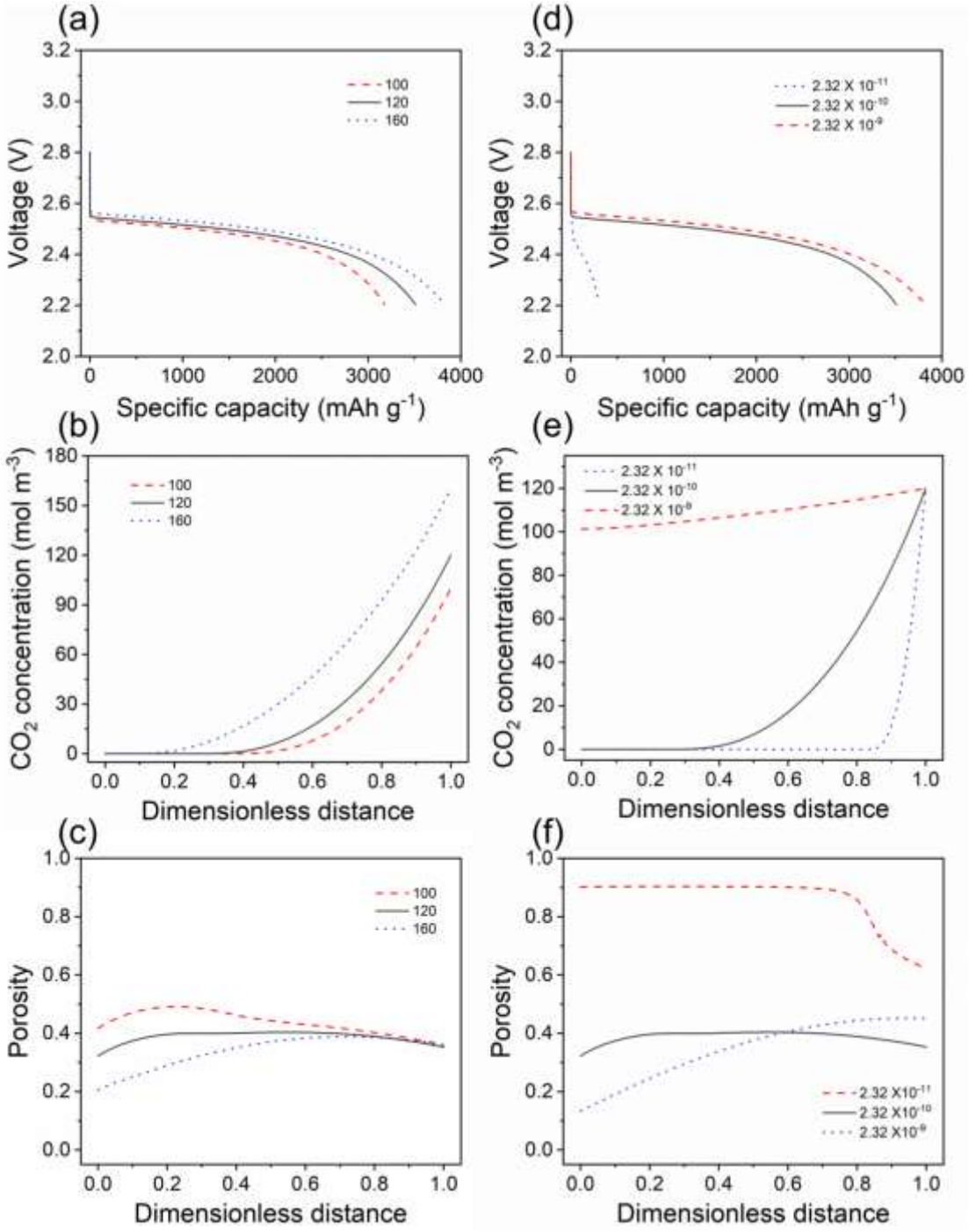

FIGURE 6 Effects of carbon dioxide (a-c) solubility and (d-f) diffusivity on the discharge performance, respectively: (a, d) discharge voltage-capacity curves; (b, e) concentration of carbon dioxide and (c, f) porosity distribution at the end of discharge.

2.4.2 Effects of carbon dioxide diffusivity

To clarify correlation CO_2 diffusivity coefficient with discharge behavior, the ratio ranges from 0.1 (2.32×10^{-11} m^2 s^{-1}) to 10 (2.32×10^{-9} m^2 s^{-1}), as shown in Fig. 6d. The corresponding capacities are significantly growing at variable speeds with the diffusivity tenfold increasing, which is ascribed to the strengthened diffusion of CO_2 to the active sites of the cathode. The specific explanation is as follows: From Fig. 6e, the higher CO_2 diffusivity leads to well-distributed concentration in the cathode at the end of discharge, which is consistent with the porosity result in Fig. 6f. In comparison with the initial value (2.32×10^{-10} m^2 s^{-1}), too large or too small values will get tightly packed deposition at the two sides. For the low diffusivity, the products are accumulated at the gas inlet side due to the high transport resistant. While for the high diffusivity, more products are generally and can achieve high utilization of the void volume of the cathode. Thus, the diffusivity can alter the distribution of products, and selecting the electrolyte with a larger diffusivity is a promising strategy to increase the discharge capacity.

2.5 Solid product component

Different from Li-O_2 batteries in which solid product is composed of Li_2O_2 only, in Li-CO_2 batteries, the product is not only lithium compound but also amorphous carbon. It is known that the discharge capacity is directly determined by how many products deposited on the cathode. Since carbon has intrinsic properties of high electrical conductivity and activated defective structure can be used as the electrode

material/catalyst,[52,53] the formed carbon may also affect the discharge behaviors. However, carbon as a component of the hybrid products has been rarely discussed yet. Herein, we assume that the volume fraction of the final discharge product (ε_s) is divided into those of solid Li_2CO_3 and carbon, which can be expressed as:

$$\varepsilon_{Li_2CO_3} = x\varepsilon_s \tag{2a}$$

$$\varepsilon_C = (1-x)\varepsilon_s \tag{2b}$$

where $\varepsilon_{Li_2CO_3}$ is the volume fraction of the solid Li_2CO_3 in the final products, and ε_C refers to the volume fraction of the solid carbon, x means the percentage value between the total products and the solid Li_2CO_3. Hence, combined with Eq. S14 and Eq. S15, the effective local surface area per unit volume of the porous cathode can be approximatively rewritten as:

$$\frac{a}{a_0} = 1 - m \cdot \left[x^{1/2} - (1-x)^{1/2} \right] \cdot \left(\frac{\varepsilon_s}{\varepsilon_0} \right)^{1/2} \tag{3}$$

where a is the active surface area per unit electrode volume ($m^2\ m^{-3}$), and a_0 is the initial value. x is restricted from 92.95% to 86.82% ($86.82\% < x < 92.95\%$) when considering the relation of products stoichiometric coefficient in Eq. 1 and assume the limiting value line of dissolution ratio of not absolutely insoluble Li_2CO_3 is nearly 50% (Schemed in Fig. 7), and m is the correction factor of volume fraction and the value is 1.432 (Supporting Information).

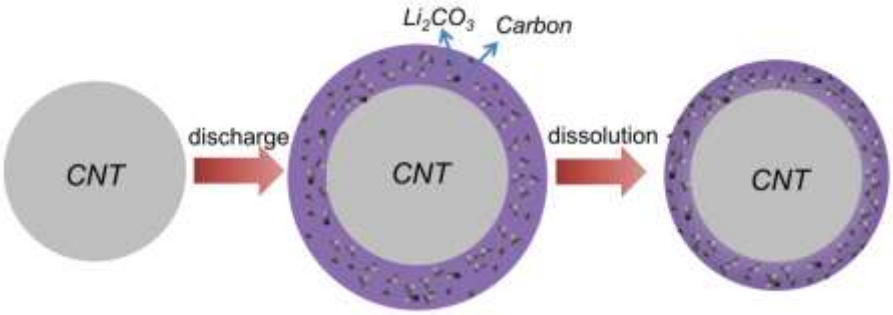

FIGURE 7 Schematic diagram of the growth of discharge product on the surface of electrode nanotube (Case 1) and the change of product component (Case 2).

The capacity increases as the volume fraction of the solid Li_2CO_3 reduces, as shown in Fig. 8a. The implication in Eq. 3 is that either less Li_2CO_3 or more carbon plays a positive role on the effective local surface area of the cathode, and the whole specific surface area degradation is originated from the enormous inactive Li_2CO_3 overwhelming to take up the pore spaces during discharge. As demonstrated in Fig. 8b, increasing the carbon content will provide more possibility to enhance CO_2 evolution reaction, since the formed carbon is regarded to provide active sites to expand the effective local surface area at a later stage. Meanwhile, it is clearly observed in Fig. 8c that with carbon increases, more discharge products are generated at two sides of cathode instead of the center. In short, the solid product component with less Li_2CO_3 or more carbon can improve the discharge performance. It should be noted that based on the hybrid product, increasing carbon is equal to decreasing Li_2CO_3. If additives with high solubility of Li_2CO_3 are put into the electrolyte, the percentage of carbon can be enlarged.

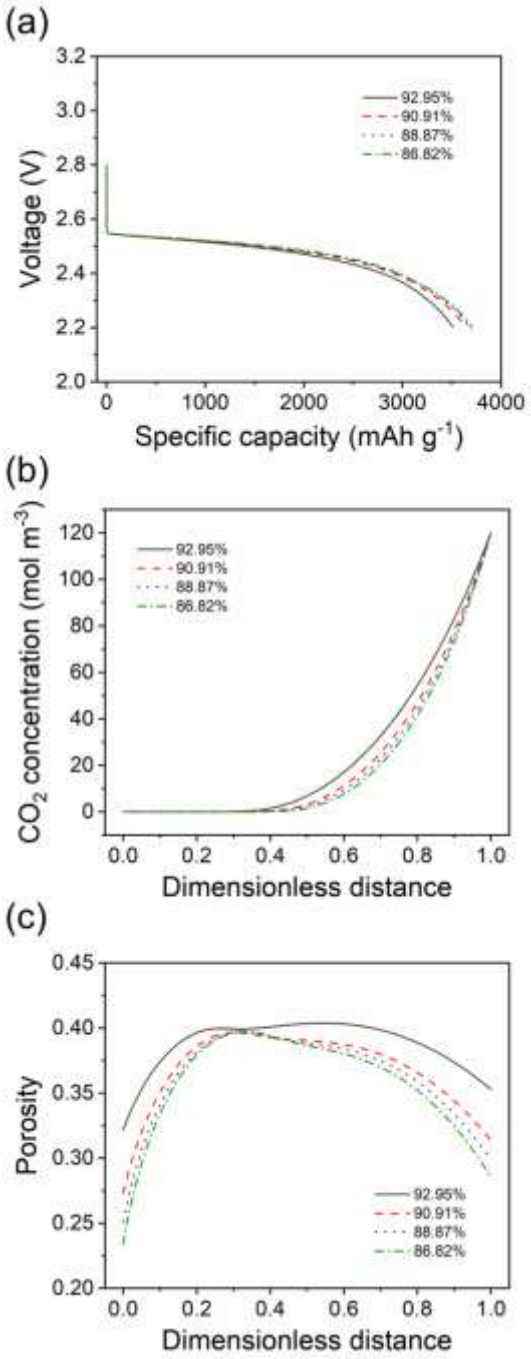

FIGURE 8 Effect of solid product component on the discharge performance: (a) discharge voltage-capacity curves; (b) concentration of carbon dioxide at the end of discharge; and (c) porosity distribution at the end of discharge.

3. CONCLUSIONS

For the newly-developed Li–CO_2 battery with the organic electrolyte, we have launched numerical analyses on the discharge performance. Based on a macroscopic continuum approach, the mathematical model has been developed and applied to describe complicated multi-physics coupling phenomena of the system. The model is firstly validated with experimental data, after which the effects of cathode geometries, electrolyte transport properties, and solid product component on the discharge performance are numerically analyzed. Compared with the solid product accumulation in a Li–O_2 battery, we reveal a different phenomenon that more products are accumulated on both sides of the cathode in Li–CO_2 batteries. Moreover, the following design strategies for performance improvements are obtained: i) Concerning the cathode geometrical properties, a thinner electrode with a larger porosity is preferred; ii) For the catalytic activity, synthesis advanced catalysts with high reaction rates are beneficial for the discharge voltage; iii) In aspect of the electrolyte selection, higher CO_2 solubility and diffusivity are more suitable to improve the energy density; iv) As to the hybrid product component, increase the carbon content or decrease the solid Li_2CO_3 content (e.g., using additives with high solubility of Li_2CO_3 in the electrolyte) can contribute to more reaction sites. This work favors to setup reasonable experimental parameters to accelerate the commercialization of Li–CO_2 batteries, and offers implications for other metal–CO_2 batteries such as Na–CO_2 and Zn–CO_2 batteries.

ACKNOWLEDGMENTS

P. Tan thanks the funding support from CAS Pioneer Hundred Talents Program and USTC Tang Scholar. M. Ni thanks the funding support from The Hong Kong Polytechnic University (G-YW2D) and a grant (Project Number: PolyU 152214/17E) from Research Grant Council, University Grants Committee, Hong Kong SAR.

REFERENCES

1. Matter JM, Stute M, Snæbjörnsdottir SÓ, Oelkers EH, Gislason SR, Aradottir ES, et al. Rapid carbon mineralization for permanent disposal ofanthropogenic carbon dioxide emissions. Science 2016;352:1312–4.
2. Peters GP, Marland G, Le Quéré C, Boden T, Canadell JG, Raupach MR. Rapid growth in CO_2 emissions after the 2008–2009 global financial crisis. Nat Clim Chang 2012;2:2–4.
3. Schrag DP. Preparing to capture carbon. Science 2007;315:812–3.
4. Gough C. State of the art in carbon dioxide capture and storage in the UK: An experts' review. Int J Greenh Gas Control 2008;2:155–68.
5. Wang C, Luo X, Luo H, Jiang DE, Li H, Dai S. Tuning the basicity of ionic liquids for equimolar CO_2 capture. Angew Chemie-Int Ed 2011;50:4918–22.
6. Erans M, Manovic V, Anthony EJ. Calcium looping sorbents for CO_2 capture. Appl Energy 2016;180:722–42.
7. Luca OR, McCrory CCL, Dalleska NF, Koval CA. The Selective Electrochemical Conversion of Preactivated CO_2 to Methane. J Electrochem Soc 2015;162:H473–6.

8. Talanquer V, Oxtoby D, Islam MF, Zhang J, Collings PJ, Yodh AG, et al. A local proton source enhances CO_2 electroreduction to CO by a molecular Fe catalyst. Science 2012;338:90–4.
9. Yang ZZ, He LN, Gao J, Liu AH, Yu B. Carbon dioxide utilization with C–N bond formation: carbon dioxide capture and subsequent conversion. Energy Environ Sci 2012;5:6602–39.
10. Zhu W, Michalsky R, Metin Ö, Lv H, Guo S, Wright CJ, et al. Monodisperse Au nanoparticles for selective electrocatalytic reduction of CO_2 to CO. J Am Chem Soc 2013;135:16833–6.
11. Yang N, Gao F, Nebel CE. Diamond decorated with copper nanoparticles for electrochemical reduction of carbon dioxide. Anal Chem 2013;85:5764–9.
12. Xu S, Das SK, Archer LA. The Li-CO_2 battery: A novel method for CO_2 capture and utilization. RSC Adv 2013;3:6656–60.
13. Li X, Yang S, Feng N, He P, Zhou H. Progress in research on Li-CO_2 batteries: Mechanism, catalyst and performance. Cuihua Xuebao/Chinese J Catal 2016;37:1016–24.
14. Chen J, Yang B, Liu B, Yan X, Xu S, Liu L, et al. Recent advances in understanding Li–CO_2 electrochemistry. Energy Environ Sci 2019;12:887–922.
15. Zhang PF, Lu YQ, Wu YJ, Yin ZW, Li JT, Zhou Y, et al. High-performance rechargeable Li-CO_2/O_2 battery with Ru/N-doped CNT catalyst. Chem Eng J 2019;363:224–33.
16. Zhou X, Zhou Z, Wei J, Xie Z, Chen Y, Zhang Q, et al. The First Introduction of

Graphene to Rechargeable Li–CO_2 Batteries. Angew Chemie Int Ed 2015;54:6550–3.

17. Qiao Y, Yi J, Wu S, Liu Y, Yang S, He P, et al. Li-CO_2 electrochemistry: a new strategy for CO_2 fixation and energy storage. Joule 2017;1:359–70.
18. Xu SM, Ren ZC, Liu X, Liang X, Wang KX, Chen JS. Carbonate decomposition: low-overpotential Li-CO_2 battery based on interlayer-confined monodisperse catalyst. Energy Storage Mater 2018;15:291–8.
19. Zhou J, Li X, Yang C, Li Y, Guo K, Cheng J, et al. A Quasi-Solid-State Flexible Fiber-Shaped Li–CO_2 Battery with Low Overpotential and High Energy Efficiency. Adv Mater 2018;31:1804439.
20. Qiao Y, Xu S, Liu Y, Dai J, Xie H, Yao Y, et al. Transient, in situ synthesis of ultrafine ruthenium nanoparticles for a high-rate Li–CO_2 battery. Energy Environ Sci 2019;12:1100–7.
21. Zhang X, Zhang Q, Zhang Z, Chen Y, Xie Z, Wei J, et al. Rechargeable Li-CO_2 batteries with carbon nanotubes as air cathodes. Chem Commun 2015;51:14636–9.
22. Qie L, Lin Y, Connell JW, Xu J, Dai L. Highly Rechargeable Lithium-CO_2 Batteries with a Boron- and Nitrogen-Codoped Holey-Graphene Cathode. Angew Chemie-Int Ed 2017;56:6970–4.
23. Yang S, Qiao Y, He P, Liu Y, Cheng Z, Zhu JJ, et al. A reversible lithium-CO_2 battery with Ru nanoparticles as a cathode catalyst. Energy Environ Sci 2017;10:972–8.

24. Zhou L, Yan W, Yu Z, He W, Liu M, Liu J, et al. Carbon Nanotube@ RuO_2 as a High Performance Catalyst for Li–CO_2 Batteries. ACS Appl Mater Interfaces 2019;11:5146–51.
25. Qi H, Sun X, Li H, Li J, Wang Y, Tamirat AG, et al. A Highly Reversible Long-Life Li–CO_2 Battery with a RuP_2-Based Catalytic Cathode. Small 2018:1803246.
26. Zhang Z, Yang C, Wu S, Wang A, Zhao L, Zhai D, et al. Exploiting Synergistic Effect by Integrating Ruthenium–Copper Nanoparticles Highly Co-Dispersed on Graphene as Efficient Air Cathodes for Li–CO_2 Batteries. Adv Energy Mater 2019;9:1802805.
27. Mao Y, Tang C, Tang Z, Xie J, Chen Z, Tu J, et al. Long-life Li–CO_2 cells with ultrafine IrO_2-decorated few-layered δ-MnO_2 enabling amorphous Li_2CO_3 growth. Energy Storage Mater 2019;18:405–13.
28. Zhang Z, Zhang Z, Liu P, Xie Y, Cao K, Zhou Z. Identification of cathode stability in Li-CO_2 batteries with Cu nanoparticles highly dispersed on N-doped graphene. J Mater Chem A 2018;6:3218–23.
29. Zhang X, Wang C, Li H, Wang XG, Chen YN, Xie Z, et al. High performance Li-CO_2 batteries with NiO-CNT cathodes. J Mater Chem A 2018;6:2792–6.
30. Hou Y, Wang J, Liu L, Liu Y, Chou S, Shi D, et al. Mo2C/CNT: An Efficient Catalyst for Rechargeable Li–CO_2 Batteries. Adv Funct Mater 2017;27:1700564.
31. Li J, Zhao H, Qi H, Sun X, Song X, Guo Z, et al. Drawing a Pencil-Trace Cathode for a High-Performance Polymer-Based Li–CO_2 Battery with Redox Mediator. Adv Funct Mater 2019;29:1806863.

32. Pipes R, Bhargav A, Manthiram A. Phenyl Disulfide Additive for Solution-Mediated Carbon Dioxide Utilization in Li–CO_2 Batteries. Adv Energy Mater 2019:1900453.
33. Tan P, Shyy W, An L, Wei ZH, Zhao TS. Electrochemistry Communications Short communication A gradient porous cathode for non-aqueous lithium-air batteries leading to a high capacity. Electrochem Commun 2014;46:111–4.
34. Jung CY, Zhao TS, An L. Modeling of lithium-oxygen batteries with the discharge product treated as a discontinuous deposit layer. J Power Sources 2015;273:440–7.
35. Liu Y, Wang R, Lyu Y, Li H, Chen L. Rechargeable Li/CO_2–O_2 (2 : 1) battery and Li/CO_2 battery. Energy Environ Sci 2014;7:677–81.
36. Tatami J, Katashima T, Komeya K, Meguro T, Wakihara T. Electrically conductive CNT-dispersed silicon nitride ceramics. J Am Ceram Soc 2005;88:2889–93.
37. Laoire CO, Mukerjee S, Abraham KM, Plichta EJ, Hendrickson MA. Influence of Nonaqueous Solvents on the Electrochemistry of Oxygen in the Rechargeable Lithium-Air Battery. J Phys Chem C 2010;114:9178–86.
38. Nyman A, Behm M, Lindbergh G. Electrochemical characterisation and modelling of the mass transport phenomena in $LiPF_6$-EC-EMC electrolyte. Electrochim Acta 2008;53:6356–65.
39. Sahapatsombut U, Cheng H, Scott K. Modelling of electrolyte degradation and cycling behaviour in a lithium-air battery. J Power Sources 2013;243:409–18.
40. Zhang JG, Wang D, Xu W, Xiao J, Williford RE. Ambient operation of Li/Air batteries. J Power Sources 2010;195:4332–7.

41. Sahapatsombut U, Cheng H, Scott K. Modelling the micro-macro homogeneous cycling behaviour of a lithium-air battery. J Power Sources 2013;227:243–53.
42. Read J, Mutolo K, Ervin M, Behl W, Wolfenstine J, Driedger A, et al. Oxygen Transport Properties of Organic Electrolytes and Performance of Lithium/Oxygen Battery. J Electrochem Soc 2003;150:A1351.
43. Liu Z, Zhang Y, Jia C, Wan H, Peng Z, Bi Y, et al. Decomposing lithium carbonate with a mobile catalyst. Nano Energy 2017;36:390–7.
44. Nanda J, Bilheux H, Voisin S, Veith GM, Archibald R, Walker L, et al. Anomalous Discharge Product Distribution in Lithium-Air Cathodes. J Phys Chem C 2012;116:8401–8.
45. Bardenhagen I, Fenske M, Fenske D, Wittstock A, Bäumer M. Distribution of discharge products inside of the lithium/oxygen battery cathode. J Power Sources 2015;299:162–9.
46. Gaya C, Yin Y, Torayev A, Mammeri Y, Franco AA. Investigation of bi-porous electrodes for lithium oxygen batteries. Electrochim Acta 2018;279:118–27.
47. Tan P, Ni M, Shao Z, Chen B, Kong W. Numerical investigation of a non-aqueous lithium-oxygen battery based on lithium superoxide as the discharge product. Appl Energy 2017;203:254–66.
48. Chen J, Zou K, Ding P, Deng J, Zha C, Hu Y, et al. Conjugated Cobalt Polyphthalocyanine as the Elastic and Reprocessable Catalyst for Flexible Li–CO_2 Batteries. Adv Mater 2019;31:1805484.
49. Zhao H, Li D, Li H, Tamirat AG, Song X, Zhang Z, et al. Ru nanosheet catalyst

supported by three-dimensional nickel foam as a binder-free cathode for Li-CO_2 batteries. Electrochim Acta 2019;299:592–9.

50. Xing Y, Yang Y, Li D, Luo M, Chen N, Ye Y, et al. Crumpled Ir Nanosheets Fully Covered on Porous Carbon Nanofibers for Long-Life Rechargeable Lithium–CO_2 Batteries. Adv Mater 2018;30:1803124.
51. Li C, Guo Z, Yang B, Liu Y, Wang Y, Xia Y. A Rechargeable Li-CO_2 Battery with a Gel Polymer Electrolyte. Angew Chemie-Int Ed 2017;56:9126–30.
52. Xing W, Li S, Du D, Wang D, Liao Y, Ge S, et al. Revealing the impacting factors of cathodic carbon catalysts for Li-CO_2 batteries in the pore-structure point of view. Electrochim Acta 2019;311:41–9.
53. Wang R, Yu X, Bai J, Li H, Huang X, Chen L, et al. Electrochemical decomposition of Li_2CO_3 in NiO-Li_2CO_3 nanocomposite thin film and powder electrodes. J Power Sources 2012;218:113–8.